Metal–Organic Frameworks

International Edition: DOI: 10.1002/anie.201802911
German Edition: DOI: 10.1002/ange.201802911

Chiral Isocamphoric Acid: Founding a Large Family of Homochiral Porous Materials

Xiang Zhao, Edward T. Nguyen, Anh N. Hong, Pingyun Feng, and Xianhui Bu**

Abstract: *Homochiral metal–organic frameworks (MOFs) are an important class of chiral solids with potential applications in chiral recognition; however, relatively few are available. Of great importance is the availability of low-cost, racemization-resistant, and versatile enantiopure building blocks. Among chiral building blocks,* D*-camphoric acid is highly prolific, yet, its trans-isomer,* L*-isocamphoric acid, has remained unknown in the entire field of solid-state materials. Its rich yet totally untapped synthetic and structural chemistry has now been investigated through the synthesis of a large family of homochiral metal isocamphorates. The first observation of diastereoisomerism in isostructural MOFs is presented. Isocamphorate has a powerful ability to create framework topologies unexpected from common inorganic building blocks, and isocamphoric acid should allow access to hundreds of new homochiral materials.*

Crystalline porous materials (CPM) play important roles in many industrially important catalytic and separation processes.[1,2] However, their use for enantioselective processes is still limited.[3] A key obstacle is the difficulty in synthesizing homochiral porous materials that integrate porosity and homochirality. While many structures adopt chiral symmetry, they tend to be grown as bulk racemates. To make bulk homochiral porous materials remains a significant challenge.

Among various forms of porous materials, MOFs have been shown to be a versatile platform for creating bulk homochirality.[4–7] A common method is incorporation of enantiopure crosslinking or pendent ligands. However, a number of issues hamper the effectiveness of this method, including limited availability and high cost of enantiopure ligands, ligand racemization, or even the loss of chiral centers (for example, dehydration of L-malic acid) under solvothermal synthesis. In this context, it is no wonder that one of the most frequently studied ligands in chiral MOFs is D-camphoric acid, abbreviated as D-cam or RS-cam herein (Figure 1).[8,9] It is the smallest readily available rigid chiral dicarboxylate. Importantly, D-cam is resistant to racemization. These attributes make D-cam an excellent building block for synthesizing homochiral MOFs.

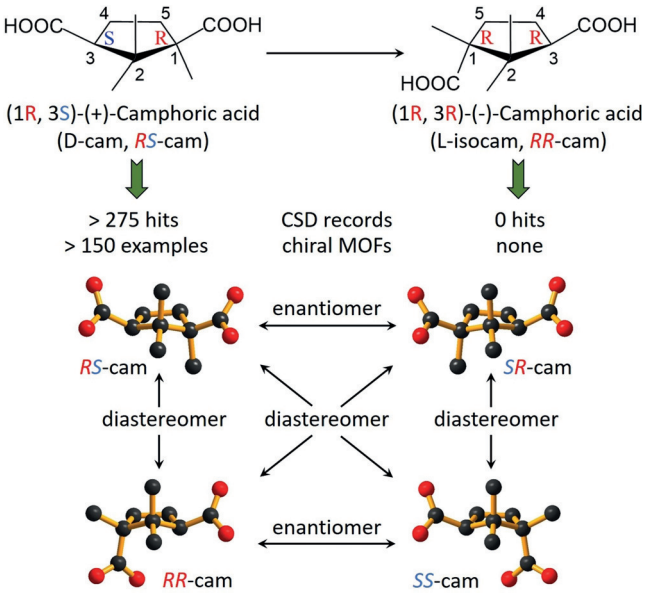

Figure 1. The naming of four stereoisomers of camphoric acid used in this study. RS-cam has been extensively studied, but no RR-cam or a compound thereof is known in the Cambridge Structural Database (CSD).

Despite the popularity of D-cam, there is an intriguing phenomenon that has so far gone unrecognized in the field of chiral MOFs: diastereoisomerism of camphoric acid (*cis*- and *trans*-camphoric acids, both of which have two chiral centers). In addition to D- and L-camphoric acids, which have the *cis*-form, there are also L- or D-isocamphoric acid, which have the *trans*-form.[10] Their nomenclature and stereoisomeric relationship are shown in Figure 1. The configuration of RR-cam, whose structure has not been studied in MOFs (or in any crystalline form) prior to this work, is quite different from the well-studied RS-cam. Thus, RR-cam provides an exciting platform in chiral chemistry, from cocrystals, supramolecular assemblies, to the development of new homochiral porous materials first reported herein.

The crystal structures for RR-cam and SS-cam and their use for the creation of a family of homochiral MOFs (Table 1) with rich compositional and structural features are presented for the first time. In some chemical systems,[9] RR-cam can replace RS-cam in its place, leading to a dramatic and long-range crystallographically ordered switching of 50% of chiral centers while preserving overall structural and topological features. In some other chemical systems, RR-cam shows much greater structural and topological diversity than RS-

[*] Dr. X. Zhao, E. T. Nguyen, A. N. Hong, Prof. X. Bu
Department of Chemistry and Biochemistry
California State University Long Beach
1250 Bellflower Boulevard, Long Beach, CA 90840 (USA)
E-mail: xianhui.bu@csulb.edu
Prof. P. Feng
Department of Chemistry, University of California
Riverside, CA 92521 (USA)
E-mail: pingyun.feng@ucr.edu
Supporting information and the ORCID identification number(s) for the author(s) of this article can be found under: https://doi.org/10.1002/anie.201802911.

Table 1: Crystal data and refinement results of new homochiral compounds synthesized herein.[11]

Code	Formula	Space group	*a* [Å]	*b* [Å]	*c* [Å]	*β*	R(F)	Flack	Net
RR-H_2cam	L-$C_{10}H_{16}O_4$	$P4_12_12$	13.8060(16)	13.8060(16)	22.455(3)	90	0.0376	0.0(8)	0-D
SS-H_2cam	D-$C_{10}H_{16}O_4$	$P4_32_12$	13.820(3)	13.820(3)	22.486(4)	90	0.0531	−0.2(9)	0-D
CPM-311-RR	$(Me_4N)In(RR\text{-cam})_2$	$P6_122$	12.361(9)	12.361(9)	37.86(3)	90	0.0431	0.026(14)	qtz
CPM-312-SR(Mg)	$Mg_3(HCOO)_4$(SR-cam)	$P3_1$	14.7922(12)	14.7922(12)	7.3144(14)	90	0.0582	0.0(3)	eta
CPM-312-RR(Mg)	$Mg_3(HCOO)_4$(RR-cam)	$P3_2$	14.8000(2)	14.8000(2)	7.4722(2)	90	0.0531	0.0(2)	eta
CPM-312-SS(Mg)	$Mg_3(HCOO)_4$(SS-cam)	$P3_1$	14.8963(14)	14.8963(14)	7.4374(7)	90	0.0468	0.11(13)	eta
CPM-312-RS(Co)	$Co_3(HCOO)_4$(RS-cam)	$P3_2$	14.8259(7)	14.8259(7)	7.4062(4)	90	0.0520	0.09(3)	eta
CPM-312-RR(Co)	$Co_3(HCOO)_4$(RR-cam)	$P3_2$	14.7363(2)	14.7363(2)	7.55860(10)	90	0.0389	0.008(10)	eta
CPM-313-RR	$Cu_2(RR\text{-cam})_2(DMF)_2$	$P6_122$	19.2517(8)	19.2517(8)	33.0352(16)	90	0.0783	0.040(14)	uon
CPM-314-RR	$Cu_2(RR\text{-cam})_2(DMEU)_2$	$P3_221$	12.2369(15)	12.2369(15)	39.188(6)	90	0.0945	0.064(13)	qtz
CPM-315-RR	$Cu_2(RR\text{-cam})_2(NMF)_{2.5}$	$P2_1$	10.698(3)	26.971(8)	11.225(3)	107.247(6)	0.0458	0.057(12)	dia
CPM-316-RR	$Cu_2(RR\text{-cam})_2(DEA)_2$	$P2_1$	10.9533(16)	13.3126(19)	13.0115(19)	108.932(4)	0.0863	0.12(2)	sql
CPM-317-RR	$Co_2(OH)$(RR-cam)-(HRR-cam)(H_2RR-cam)$_2$	$P2_1$	13.525(5)	12.735(4)	14.421(5)	112.957(7)	0.0710	0.00(2)	ecu
CPM-332-RR	$Cu_2(RR\text{-cam})_2$(bpy)	$P2_1$	13.317(4)	12.797(4)	13.946(4)	90.965(7)	0.0841	0.07(3)	pcu

cam and can lead to materials with greater porosity. One striking feature of RR-cam is its powerful ability to form 4-connected intrinsically chiral 3D framework.

CPM-311 and CPM-312 families of materials, in all four RS-, SR-, RR-, and SS-homochiral forms, demonstrate an unprecedented solid-state phenomenon: enantiomeric, diastereomeric, and isoreticular MOFs. There are many examples of isoreticular MOFs, however, they are rarely diastereomeric at molecular level. It is thus a truly intriguing solid-state phenomenon when diastereomers can form isoreticular MOFs with nearly identical crystal structures. It means that it is now possible to switch the chiral environment by replacing an enantiopure ligand with its chiral diastereomer without altering its crystal structure and framework topology. In this work, we were able to accomplish this type of chirality switching when the chiral ligand is either a crosslinking ligand or a pendant ligand.

CPM-311-RR, formulated as $(Me_4N)In(RR\text{-cam})_2$ with RR-cam as crosslinker, features uninodal 4-connected quartz (**qtz**) net with four RR-cam ligands chelating to the indium monomer (Figure 2a). The structure integrates three types of chirality features: the 0-D chirality of RR-cam, the intrinsic 3D chiral **qtz** net, and 1D absolute helicity. CPM-311-RR and its diastereomeric CPM-311-RS have the same structure, with the only difference being the chirality around one of the two chiral centers (C3; Figure 2a). Mimicking the stereoisomer concept in molecules, herein we name these isoreticular MOFs as stereoiso-MOFs, including diastereo-MOFs and enantio-MOFs.

CPM-312 is an excellent example that illustrates the close correlation between an individual chiral center and the overall absolute helicity. Specifically, a change in the chirality of C3 does not change the absolute helicity, while a change in the chirality of C1 switches the absolute helicity of Mg^{2+}-format helix to which chiral camphorates are attached. CPM-312 has honeycomb channels with a Mg^{2+}-format backbone. RR-cam acts as an auxiliary ligand attached on the wall of the hexagonal channel (Figure 2b). Together with CPM-312-SS, CPM-312-RS, and CPM-312-SR, they form another family of stereoisomeric MOFs with the same structure, but different chiral properties. These four CPM-312 compounds can be understood as internal pore-surface modification with different chiral ligands on the same primary framework. CPM-312 adopts the chiral **eta** net with Mg-HCOO helices (3_1 or 3_2). Interestingly, there is a relationship between the helix and the auxiliary ligands. When the auxiliary ligand is RS-cam or RR-cam, the inorganic chains adopt 3_2 helix. However, when the auxiliary ligand is SR-cam or SS-cam, the chains adopt 3_1 helix. This shows that the absolute helicity of chain is controlled by the stereochemistry around C1 of camphorates.

CPM-313-RR to CPM-316-RR, based on copper paddlewheel dimers, illustrate that diastereoisomerization of the chiral linker (transition from *cis* RS-cam to *trans* RR-cam) results in greater structural diversity (Figure 3). Moreover, these materials demonstrate the powerful ability of RR-cam to construct various 4-connected frameworks, even from square-planar nodes. By flipping one chiral center on the cyclopentane ring, RR-cam gives dramatically different configurations from RS-cam. Such a difference is further amplified when coordinated to metal nodes. As a result, the relative orientation between adjacent metal nodes is affected, leading to various framework types. It is worth noting that copper paddlewheel is a planar 4-connected node and has difficulty forming 3D frameworks with dicarboxylate, in the absence of auxiliary ligands such as 4,4′-bipyridine. RS-cam itself tends to form a square net with copper dimers. In contrast, by using its diastereoisomer RR-cam, we have made several copper-dimer-based phases in different topologies. A prominent example is CPM-313-RR which exhibits a very rare intrinsically chiral 4-connected net (**uon**). Adding to the structural diversity, the formation of these 4-connected nets are sensitive to the solvent used. Four structure types have been obtained in DMF (CPM-313, **uon**), DMEU (CPM-314, **qtz**), NMF (CPM-315, **dia**), and DEA (CPM-316, **sql**), respectively. In comparison, the assembly between RS-cam and copper dimer is not much sensitive to the reaction conditions. This show that RR-cam can serve as a platform for exploring the synthetic and structural chemistry of homochiral structures. The versatility of RR-cam was observed again in CPM-317-RR, a cobalt compound. CPM-317-RR features V-shaped cobalt dimers (Supporting Information, Figure S6) connected by eight RR-cam to form the **ecu** net.

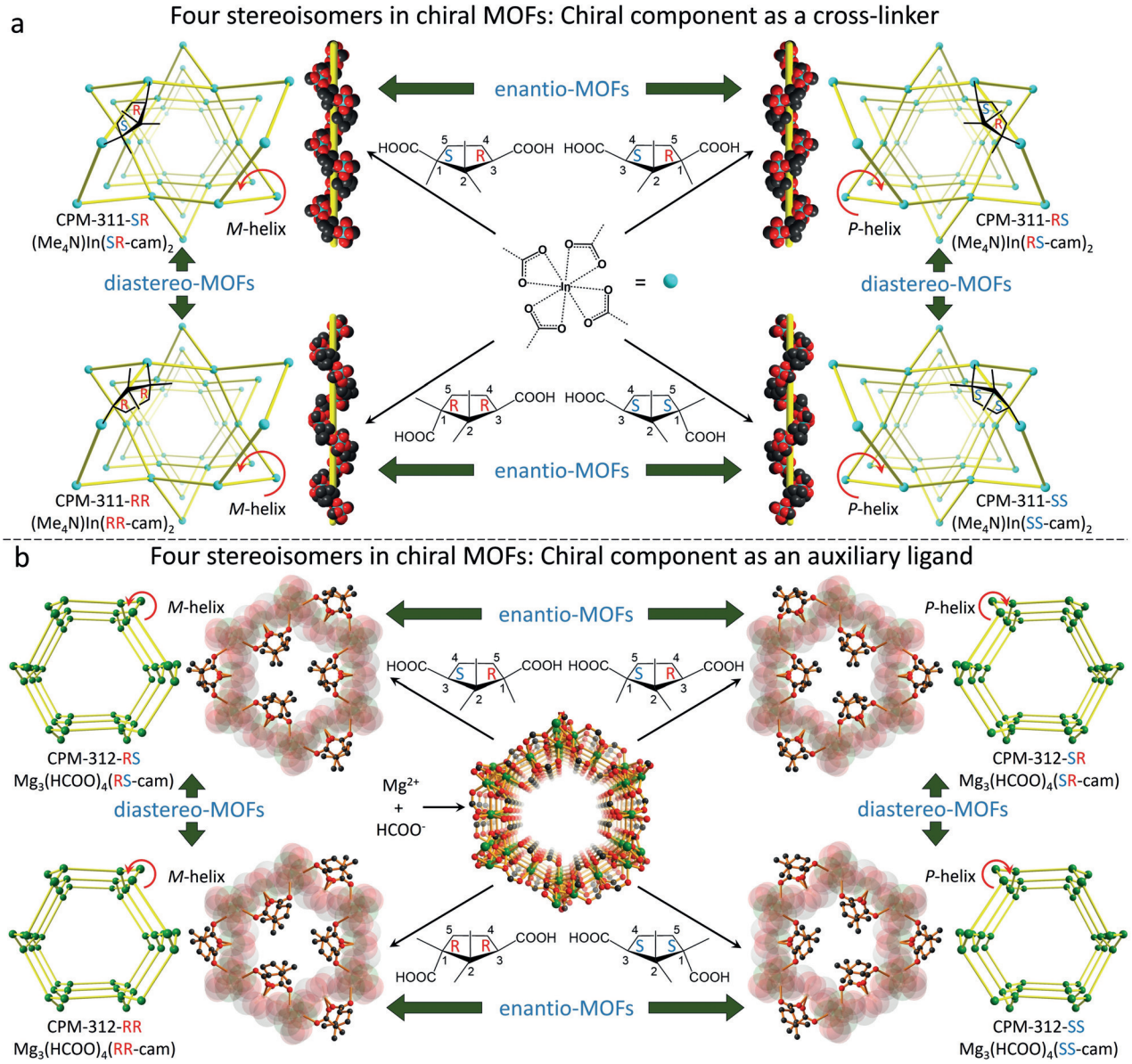

Figure 2. Chirality switching without topological change illustrated by two types of stereoisomerization in MOFs. a) In CPM-311, the crystallization between the monomeric $In(COO)_4$ and four stereoisomers of camphoric acid leads to the same quartz type structure. b) In CPM-312, the crystallization between magnesium and formate form a honeycomb structure, with camphoric acid as a chiral pendant on the wall.

CPM-331-RS and CPM-332-RR further illustrate the difference between RS-cam and RR-cam. CPM-331 and CPM-332 are isomers with the same formula of $Cu_2(cam)_2$-(bpy). In both structures, the copper dimers are connected by camphorates to form the square layer structure (Figure 4a). However, the chiral configuration around one of the stereocenters (C3) is different. When the layers are pillared by 4,4′-bipyridine ligand, two distinct 3D structures with uninodal 6-connected nets are obtained. CPM-331-RS features the **rob** topology with the wavy sheet while CPM-332 features the **pcu** topology with the flat sheet. An evaluation from Platon program shows that in CPM-331-RS has little accessible pore, while the void space is about 44.7% in CPM-332-RR. A gas sorption study further supports the difference (Figure 4b). The BET surface area of both compounds were determined by N_2 sorption at 77 K. CPM-332-RR has a BET surface area of about 216.02 $m^2 g^{-1}$ while CPM-331-RS is 16.43 $m^2 g^{-1}$. The micropore volume in CPM-332-RR is 0.106 $cm^3 g^{-1}$ and is negligible in CPM-331-RS. Furthermore, their H_2 sorption at 77 K and 1 atm is 85.0 $cm^3 g^{-1}$ and 27.2 $cm^3 g^{-1}$, respectively.

CPM-332-RR is fluorescent with strong emission at about 365 nm (excitation at 286 nm). Its pore opening allows chiral organic guests to enter the voids and chiral recognition can be achieved due to different degrees of fluorescent quenching. Herein, the fluorescent quenching by (*R*)-/(*S*)-α-ethylbenzylamine (EBA) was studied. A stable suspension of CPM-332-RR was prepared by dispersing crushed crystalline sample in acetonitrile followed by vigorous stirring overnight. Then the (*R*)- or (*S*)- enantiomer of EBA was added to the suspension. Fluorescence emission spectra were monitored with incre-

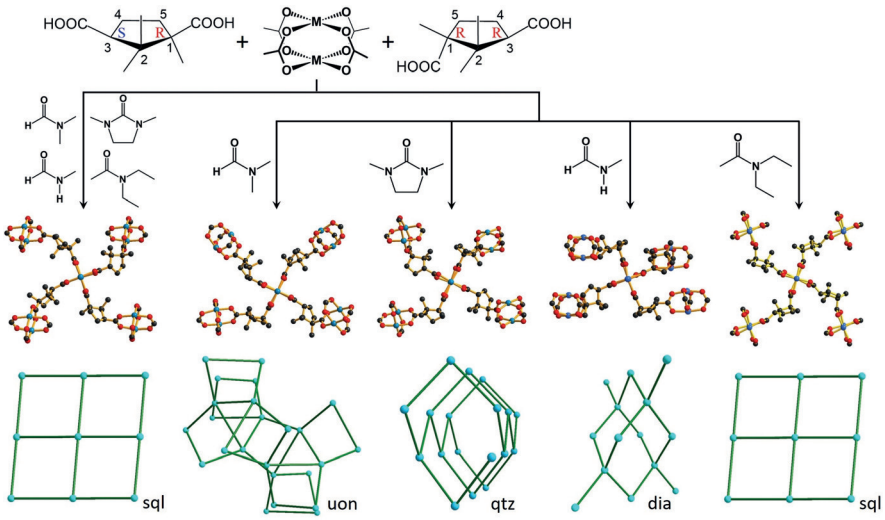

Figure 3. Increased structural diversity owing to diastereoisomerization. The crystallization between copper dimers and RS-cam leads to the 2D **sql** net. In contrast, by replacing RS-cam with its diastereomer RR-cam, a number of chiral topologies can be obtained by using different solvents.

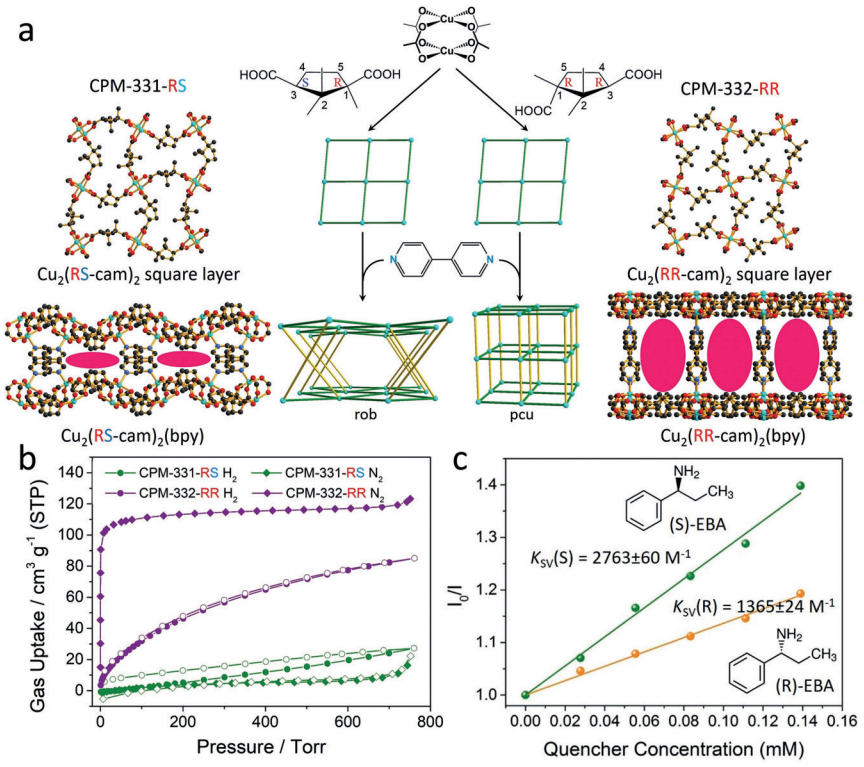

Figure 4. a) Stereoisomerization-induced pore opening. With similar building scheme and square-layer building unit, but with different spatial configuration, RS-cam and RR-cam lead to different 3D structures when the layers are pillared by bipyridine, resulting in CPM-331-RS and CPM-332-RR, respectively. b) CPM-332-RR shows dramatically enhanced porosity. c) Stern–Volmer plots of the fluorescence emission of CPM-332-RR quenched by (*R*)- & (*S*)-α-ethylbenzylamine, respectively.

mental addition of chiral compounds. As expected, fluorescence quenching was observed upon the addition of EBA, however at a different quenching rate (Figure 4c). The quenching plot at low quencher concentration follows the Stern–Volmer relationship. It was calculated that the K_{SV} for (*S*)-EBA is $2763 \pm 60\,M^{-1}$ and K_{SV} for (*R*)-EBA is $1365 \pm 24\,M^{-1}$. The corresponding enantioselectivity in terms of quenching ratio [$QR = K_{SV}(S)/K_{SV}(R)$] is about 2.02. The above result indicates that RR-cam based homochiral materials are promising chiral host for enantioselective adsorption and recognition.

In conclusion, we have created a novel family of homochiral metal–organic frameworks that exhibit abundant compositional, structural, topological, and chiral features. For the first time, we have created a full family of stereoisomeric MOFs including enantiomeric, diastereomeric, and isoreticular MOFs, which enable the selective switching of chirality in isoreticular frameworks. It is expected that starting from this study, a large family of homochiral materials can be created and new chiral phenomena will be discovered. New RR-cam derived homochiral materials can serve as valuable low-cost candidates for enantioselective applications such as chiral separation. Furthermore, this work has revealed a new general route to create homochiral materials by creating new chiral ligand from chiral conversion of pre-existing chiral ligand. This method can be applied to other chiral ligands with multiple chiral centers. Clearly, the introduction of a new enantiopure ligand, especially if cheap and readily available, can generate numerous new opportunities in synthesis, structures, and applications of homochiral materials.

Acknowledgements

This work was supported by National Science Foundation, Division of Materials Research, under Award #1309347 (X.B.). X.B. thanks the RSCA award from CSULB.

Conflict of interest

The authors declare no conflict of interest.

Keywords: camphoric acid · chiral ligands · homochiral porous materials · isocamphoric acid · metal–organic frameworks

How to cite: *Angew. Chem. Int. Ed.* **2018**, *57*, 7101 – 7105
Angew. Chem. **2018**, *130*, 7219 – 7223

[1] a) M. I. H. Mohideen, B. Xiao, P. S. Wheatley, A. C. McKinlay, Y. Li, A. M. Z. Slawin, D. W. Aldous, N. F. Cessford, T. Düren, X. Zhao, R. Gill, K. M. Thomas, J. M. Griffin, S. E. Ashbrook, R. E. Morris, *Nat. Chem.* **2011**, *3*, 304; b) H.-S. Lu, L. Bai, W.-W. Xiong, P. Li, J. Ding, G. Zhang, T. Wu, Y. Zhao, J.-M. Lee, Y. Yang, B. Geng, Q. Zhang, *Inorg. Chem.* **2014**, *53*, 8529; c) D. Banerjee, A. Cairns, J. Liu, R. K. Motkuri, S. K. Nune, C. A. Fernandez, R. Krishna, D. M. Strachan, P. K. Thallapally, *Acc. Chem. Res.* **2015**, *48*, 211; d) L. Jiao, Y. Wang, H.-L. Jiang, Q. Xu, *Adv. Mater.* **2018**, DOI: https://doi.org/10.1002/adma.201703663.

[2] a) B. Li, H. M. Wen, Y. Cui, W. Zhou, G. Qian, B. Chen, *Adv. Mater.* **2016**, *28*, 8819; b) J. Zhao, Y. Wang, W. Dong, Y. Wu, D. Li, B. Liu, Q. Zhang, *Chem. Commun.* **2015**, *51*, 9479; c) C. Wang, D. Liu, W. Lin, *J. Am. Chem. Soc.* **2013**, *135*, 13222; d) J. Gao, J. Miao, P.-Z. Li, W. Y. Teng, L. Yang, Y. Zhao, B. Liu, Q. Zhang, *Chem. Commun.* **2014**, *50*, 3786; e) L.-D. Lin, X.-X. Li, Y.-J. Qi, X. Ma, S.-T. Zheng, *Inorg. Chem.* **2017**, *56*, 4635; f) J.-D. Xiao, L. Han, J. Luo, S.-H. Yu, H.-L. Jiang, *Angew. Chem. Int. Ed.* **2018**, *57*, 1103; *Angew. Chem.* **2018**, *130*, 1115; g) D. Banerjee, C. M. Simon, A. M. Plonka, R. K. Motkuri, J. Liu, X. Chen, B. Smit, J. B. Parise, M. Haranczyk, P. K. Thallapally, *Nat. Commun.* **2016**, *7*, 11831.

[3] a) J. S. Seo, D. Whang, H. Lee, S. I. Jun, J. Oh, Y. J. Jeon, K. Kim, *Nature* **2000**, *404*, 982; b) L. Ma, J. M. Falkowski, C. Abney, W. Lin, *Nat. Chem.* **2010**, *2*, 838; c) Y. Liu, W. Xuan, Y. Cui, *Adv. Mater.* **2010**, *22*, 4112; d) H.-L. Qian, C.-X. Yang, X.-P. Yan, *Nat. Commun.* **2016**, *7*, 12104; e) S.-C. Xiang, Z. Zhang, C.-G. Zhao, K. Hong, X. Zhao, D.-R. Ding, M.-H. Xie, C.-D. Wu, M. C. Das, R. Gill, K. M. Thomas, B. Chen, *Nat. Commun.* **2011**, *2*, 204; f) S.-Y. Zhang, C.-X. Yang, W. Shi, X.-P. Yan, P. Cheng, L. Wojtas, M. J. Zaworotko, *Chem* **2017**, *3*, 281; g) Q. Xia, Z. Li, C. Tan, Y. Liu, W. Gong, Y. Cui, *J. Am. Chem. Soc.* **2017**, *139*, 8259.

[4] a) R. E. Morris, X. Bu, *Nat. Chem.* **2010**, *2*, 353; b) Z. Lin, A. M. Z. Slawin, R. E. Morris, *J. Am. Chem. Soc.* **2007**, *129*, 4880; c) L. Ma, C. Abney, W. Lin, *Chem. Soc. Rev.* **2009**, *38*, 1248; d) D. Bradshaw, J. B. Claridge, E. J. Cussen, T. J. Prior, M. J. Rosseinsky, *Acc. Chem. Res.* **2005**, *38*, 273; e) M. Xue, B. Li, S. Qiu, B. Chen, *Mater. Today* **2016**, *19*, 503.

[5] a) Y. Peng, T. Gong, K. Zhang, X. Lin, Y. Liu, J. Jiang, Y. Cui, *Nat. Commun.* **2014**, *5*, 4406; b) K. Wu, K. Li, Y.-J. Hou, M. Pan, L.-Y. Zhang, L. Chen, C.-Y. Su, *Nat. Commun.* **2016**, *7*, 10487; c) S. Lee, E. A. Kapustin, O. M. Yaghi, *Science* **2016**, *353*, 808.

[6] a) S.-Y. Zhang, D. Li, D. Guo, H. Zhang, W. Shi, P. Cheng, L. Wojtas, M. J. Zaworotko, *J. Am. Chem. Soc.* **2015**, *137*, 15406; b) D. Luo, X.-Z. Wang, C. Yang, X.-P. Zhou, D. Li, *J. Am. Chem. Soc.* **2018**, *140*, 118; c) P. Wu, C. He, J. Wang, X. Peng, X. Li, Y. An, C. Duan, *J. Am. Chem. Soc.* **2012**, *134*, 14991; d) Y. Zhang, J. Guo, L. Shi, Y. Zhu, K. Hou, Y. Zheng, Z. Tang, *Sci. Adv.* **2017**, *3*, e1701162.

[7] a) P. Li, Y. He, J. Guang, L. Weng, J. C.-G. Zhao, S. Xiang, B. Chen, *J. Am. Chem. Soc.* **2014**, *136*, 547; b) M. Padmanaban, P. Müller, C. Lieder, K. Gedrich, R. Grünker, V. Bon, I. Senkovska, S. Baumgärtner, S. Opelt, S. Paasch, E. Brunner, F. Glorius, E. Klemm, S. Kaskel, *Chem. Commun.* **2011**, *47*, 12089; c) M. Zhang, Z.-J. Pu, X.-L. Chen, X.-L. Gong, A.-X. Zhu, L.-M. Yuan, *Chem. Commun.* **2013**, *49*, 5201; d) H. Wang, Z. Chang, Y. Li, R.-M. Wen, X.-H. Bu, *Chem. Commun.* **2013**, *49*, 6659.

[8] Z.-G. Gu, C. Zhan, J. Zhang, X. Bu, *Chem. Soc. Rev.* **2016**, *45*, 3122.

[9] a) J. Zhang, S. Chen, A. Zingiryan, X. Bu, *J. Am. Chem. Soc.* **2008**, *130*, 17246; b) J. Zhang, S. M. Chen, H. Valle, M. Wong, C. Austria, M. Cruz, X. Bu, *J. Am. Chem. Soc.* **2007**, *129*, 14168; c) J. Zhang, Y.-G. Yao, X. Bu, *Chem. Mater.* **2007**, *19*, 5083; d) Z. Ju, G. Liu, Y.-S. Chen, D. Yuan, B. Chen, *Chem. Eur. J.* **2017**, *23*, 4774.

[10] W. A. Noyes, L. Knight, *J. Am. Chem. Soc.* **1910**, *32*, 1669.

[11] CCDC 1827976 – 1827989 contain the supplementary crystallographic data for this paper. These data are provided free of charge by The Cambridge Crystallographic Data Centre.

Manuscript received: March 8, 2018
Revised manuscript received: April 11, 2018
Version of record online: May 17, 2018

